

青藏高原拉萨地块中西部超钾质岩 Ca-Mg 同位素特征及其地质意义

刘峪菲^{1,2)}, 许继峰^{3,1)}, 张兆峰¹⁾, 王桂琴¹⁾, 陈建林¹⁾,
黄丰^{3,1)}, 祝红丽^{1,2)}, 刘芳^{1,2)}

1) 中国科学院广州地球化学研究所, 同位素地球化学国家重点实验室, 广州, 510640;
2) 中国科学院大学, 北京, 100049; 3) 中国地质大学(北京)地球科学与资源学院, 北京, 100083

内容提要:本文通过对青藏高原拉萨地块中西部米巴勒及麦嘎地区的 8 个超钾质岩样品进行钙、镁同位素测定, 在排除了风化作用、地壳混染、分离结晶及部分熔融等后期作用对超钾质岩钙、镁同位素组成的影响后, 可能有来自俯冲新特提斯洋壳的碳酸盐沉积物交代超钾质岩的地幔源区。本文研究表明, 米巴勒及麦嘎地区超钾质岩的 $\delta^{44}\text{Ca} = 0.59 \sim 0.75$ (平均值为 0.68 ± 0.04), 明显低于上地幔(1.05 ± 0.04)、硅酸盐地球值(0.94 ± 0.05)及已发表的岩浆岩值(0.80 ± 0.10), 指示出超钾质岩源区含有低 $\delta^{44}\text{Ca}$ 组成的物质加入; Mg 同位素组成 $\delta^{26}\text{Mg} = -0.33 \sim -0.24$ (平均值为 -0.29 ± 0.03), 比上地幔值(-0.25 ± 0.07)略低, 但在误差范围内一致。超钾质岩的钙、镁同位素之间还存在一定的正相关性, 进一步指示其源区有同时具有低钙、低镁同位素组成的物质加入。通过对拉萨地块构造演化过程的识别, 笔者认为这些具有低钙、低镁同位素组成的物质极有可能是来自俯冲新特提斯洋壳的碳酸盐沉积物。

关键词:拉萨地块; 超钾质岩; Ca-Mg 同位素; 地幔源区; 特提斯俯冲

印度板块与欧亚板块发生碰撞后, 在青藏高原拉萨地块内形成了一套钾质—超钾质火山岩, 这类后碰撞期形成的岩石不仅为青藏高原深部的地幔活动提供了线索, 同时对研究青藏高原形成演化及动力学过程提供了重要的岩石学依据(Turner et al., 1996; Miller et al., 1999; Ding Lin et al., 2003, 2006; Williams et al., 2004; Zhao Zhidan et al., 2006, 2008, 2009; Gao Yongfeng et al., 2007; Chen Jianlin et al., 2007, 2008; Sun Chenguang et al., 2007, 2008; Tommasini et al., 2011; Tian Shihong et al., 2012; Guo Zhengfu et al., 2013, 2015; Hébert et al., 2014; Liu Dong et al., 2014a, 2014b, 2015; Huang Feng et al., 2015)。

自 20 世纪 70 年代起对拉萨地块超钾质岩石的研究已取得了不少成果, 基本确定其来源于一个富集的地幔源区(Turner et al., 1996; Miller et al., 1999; Williams et al., 2004; Zhao Zhidan et al.,

2009; Liu Dong et al., 2014a, 2014b, 2015; Guo Zhengfu et al., 2015; Huang Feng et al., 2015)。然而, 关于超钾质岩的形成过程及可能的富集地幔源区组成仍未得到一致的认识。目前对于超钾质岩富集地幔源区的形成主要存在两种观点, 一部分学者认为是由向北俯冲的印度大陆地壳物质交代拉萨地块下部的地幔形成(Ding Lin et al., 2003, 2006; Sun Chenguang et al., 2007, 2008; Zhao Zhidan et al., 2009; Tian Shihong et al., 2012; Guo Zhengfu et al., 2015); 另一部分学者认为由陆陆碰撞前俯冲的新特提斯洋壳物质加入到拉萨地块下部地幔交代形成(Gao Yongfeng et al., 2007; Tommasini et al., 2011; Liu Dong et al., 2014a)。尽管近年来有少量学者提出拉萨地块本身的古老地壳物质对超钾质岩的形成也具有一定贡献(Hébert et al., 2014; Liu Dong et al., 2014a), 然而这些古老基底物质还未得到很好的识别, 对超钾质岩富集

注: 本文为国家自然科学基金项目(编号 41373007、41603033), 国家重点基础研究发展计划(编号 2016YFC0600304)和博士后创新人才支持计划(编号 BX201700213)联合资助成果。

收稿日期: 2017-08-22; 改回日期: 2017-09-06; 责任编辑: 周健。

作者简介: 刘峪菲, 女, 1990 年生。博士研究生, 同位素地球化学专业。Email: liuyufei@gig.ac.cn。通讯作者: 许继峰, 男, 1963 年生。研究员, 主要从事岩石地球化学研究。Email: jifengxu@cugb.edu.cn。

地幔源区的争议焦点仍然是:①新特提斯洋壳沉积物或是②印度陆壳物质加入地幔导致超钾质岩的形成。已有的研究中,多以全岩主、微量元素,Sr-Nd-Pb 等放射性同位素地球化学特征对其源区进行判别,但这些反映的往往是岩石最终产出时具有的地球化学特征,并不能指示源区物质的不同贡献。因此,仍需要有更为精确的示踪手段来识别富集地幔源区的组成。

随着近年来仪器分析技术的发展,诸如 Ca、Mg 同位素等先前受技术限制的非传统稳定同位素逐渐应用到地球化学研究领域中。Ca、Mg 同位素在自然界中存在明显的同位素分馏,其在上地幔和海相沉积碳酸盐之间具有明显不同的同位素组成特征,为使用 Ca、Mg 同位素识别受海相碳酸盐改造的地幔物质组成提供了可能。目前已有一些研究采用 Ca 或 Mg 同位素示踪洋壳俯冲地区及俯冲带相关的源区特征(Huang Shichun et al., 2011; John et al., 2012; Wang Shuijiong et al., 2014; Liu Dong et al., 2015; Hu Yan et al., 2017; Liu Pingping et al., 2017; Su Benxun et al., 2017),如 Huang Shichun et al. (2011)通过对夏威夷拉斑玄武岩 Ca 同位素组成的研究,结合其微量元素特征识别出约 4% 的古老的碳酸盐沉积物混入夏威夷玄武岩的地幔源区。但目前同时使用这两种同位素进行源区示踪的研究仍然有限。

基于 Ca-Mg 同位素在识别地幔源区的独特优势,本文首次对拉萨地块米巴勒和麦嘎地区的超钾质岩进行了 Ca-Mg 同位素分析,并结合超钾质岩的主、微量元素地球化学特征对其富集地幔源区可能的物质组成进行探讨,一方面填补了超钾质岩 Ca 同位素组成研究的空白,另一方面通过 Ca-Mg 联合示踪为识别区域内超钾质岩的地幔源区特征提供了新的数据基础。

1 区域地质背景及样品特征

古生代以来,随着古老特提斯洋盆的闭合,欧亚大陆南缘逐渐形成了由东西向延伸的拉萨地块、羌塘地块、松潘-甘孜地块及多条蛇绿混杂岩带拼合而成的青藏高原(Dewey et al., 1988; Yin An and Harrison, 2000; Zhu Dichen et al., 2013; Xu Zhiqin et al., 2016)。拉萨地块位于青藏高原最南端,北部经班公错-怒江缝合带与羌塘地块相连;南部经喜马拉雅-雅鲁藏布江缝合带与喜马拉雅造山带相连(图 1a)(Xu Jifeng and Castillo, 2004;

Wang Baodi et al., 2014; Guo Zhengfu et al., 2015)。受印度板块与欧亚板块碰撞后陆内伸展作用的影响,中新世时期拉萨地块内广泛形成了一套钾质—超钾质岩石,其出露面积较小,以熔岩、岩脉等形式为主,多沿南北向地堑或南北向延长湖泊分布(图 1a) (Zhao Zhidan et al., 2009; Guo Zhengfu et al., 2013, 2015; Wang Baodi et al., 2014; Huang Feng et al., 2015)。

本次研究选取了米巴勒和麦嘎地区采集的 8 个超钾质岩样品,采样地点见图 1b、c。米巴勒位于拉萨地块中部,紧靠当惹雍错-许如错地堑,区域上主要出露白垩纪火山-沉积岩组合和新生代林子宗火山岩,南北部均有石炭纪一二叠纪灰岩-砂岩组合和侏罗纪花岗岩类侵入体出露(图 1b)(Ding Lin et al., 2003; Guo Zhengfu et al., 2013; Huang Feng et al., 2015)。米巴勒超钾质岩以喷出岩形式覆盖在新生代林子宗火山岩及白垩纪火山-沉积岩之上,主要沿当惹雍错-许如错地堑两侧分布,形成时间大致在 12.6~19Ma(Liao Siping et al., 2002; Xie Guogang et al., 2004; Gao Yongfeng et al., 2007; Guo Zhengfu et al., 2013)。麦嘎则位于拉萨地块西部,主要出露大量石炭纪一二叠纪灰岩-砂岩组合及侏罗纪花岗岩类侵入体,北部少量出现新生代林子宗火山岩(图 1c)。麦嘎超钾质岩主要以熔岩丘形式覆盖在石炭纪一二叠纪灰岩-砂岩组合上,形成时间约为 17Ma(Ding Lin, 2006; Chen Jianlin, 2007)。

米巴勒、麦嘎超钾质岩主要岩石类型是粗玄岩、粗面岩及粗安岩,普遍具有斑状结构,斑晶大小可达 1~2mm,多为橄榄石、透辉石、钾长石、金云母、黑云母、角闪石及少量副矿物如铁钛氧化物、磷灰石及锆石等矿物,而基质具有粗面结构,主要矿物为钾长石、黑云母、玻璃及不透明矿物微晶。详细的矿物学特征可参见已发表的相关研究(Zhao Zhidan et al., 2006, 2009; Gao Yongfeng et al., 2007; Chen Jianlin et al., 2007; Guo Zhengfu et al., 2013, 2015; Huang Feng et al., 2015)。

2 分析方法

本文所有岩石样品均已剥除外部风化壳,取出的新鲜样品研磨至 200 目粉末用于同位素分析。样品的 Ca、Mg 同位素化学分离是在中国科学院广州地球化学研究所(GIGCAS)同位素地球化学国家重点实验室完成,Ca 同位素测定在中国科学院广州地球化学研究所地球化学国家重点实验室 Triton

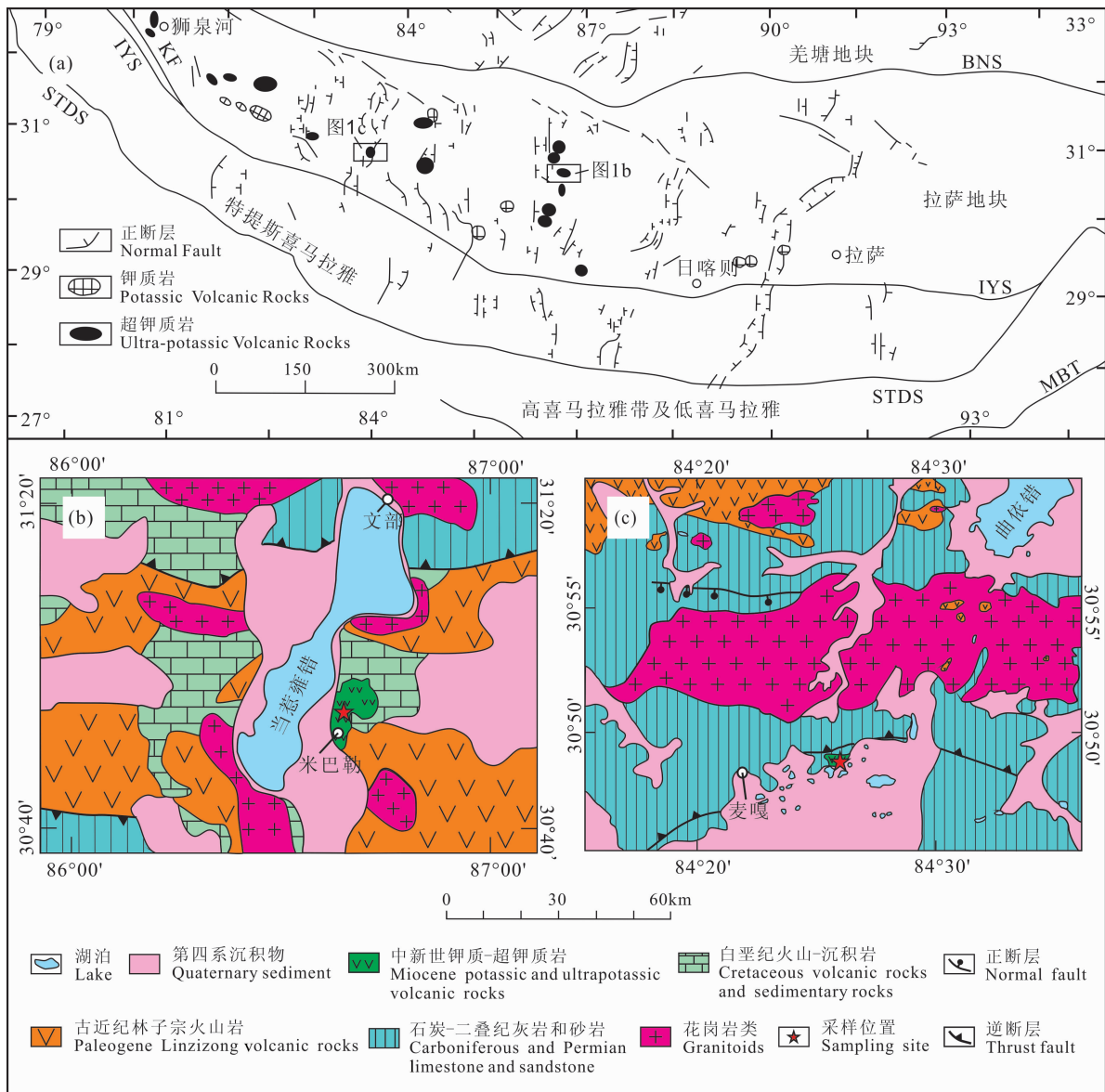


图 1 拉萨地块超钾质岩的区域地质简图

Fig. 1 Sketch geological map of ultra-potassic volcanic rocks in Lhasa Terrane

(a)—拉萨地块超钾质岩分布简图(据 Zhao Zhidan et al., 2006; Chen Jianlin et al., 2008 修改);(b)—米巴勒地区区域地质图(据 Ding Lin et al., 2003; Chen Jianlin et al., 2010; Guo Zhengfu et al., 2013; Huang Feng et al., 2015 修改);(c)—麦嘎地区区域地质图(据 Huang Feng et al., 2015 修改);BNS—班公错-怒江缝合带;KF—喀喇昆仑断裂带;IYS—印度-雅鲁藏布江缝合带;STDS—藏南拆离系;MBT—主边界断裂

(a)—The distributions of ultra-potassic volcanic rocks in Lhasa Terrane (modified from Zhao Zhidan, 2006; Chen Jianlin, 2008); (b)—simplified geological map of Mibale area (modified from Ding Lin et al., 2003; Chen Jianlin et al., 2010; Guo Zhengfu et al., 2013; Huang Feng et al., 2015); (c)—simplified geological map of Maiga area (modified from Huang Feng et al., 2015); BNS—Banggongcuo-Nujiang suture zone; KF—Karakorum fault; IYS—Indus-Yarlung Zangbo suture zone; STDS—southern Tibetan detachment system; MBT—main boundary fault

TIMS 上完成, Mg 同位素测定在中国科技大学 (USTC)壳幔物质与环境重点实验室 Neptune Plus MC-ICP-MS 上完成。

2.1 样品溶解

样品的化学前处理工作均在超净实验室环境下

完成。对于硅酸盐样品,称取 20~50mg 全岩粉末 (200 目) 样品,依照 3:1 的比例加入二次纯化的浓 HF 及浓 HNO₃,摇匀后放在 90℃ 电热板上加热一周后开盖蒸干。之后用王水处理以排除可能存在的有机物,蒸干后再加入 3 mol/L HCl 用以溶解样品

中的 CaF_2 , 重复这一步骤直至完全溶解。对于碳酸盐样品只需在称取样品后加入 2~4 mol/L HCl 溶样, 至样品完全溶解即可。最终样品蒸干后针对不同同位素体系要求进行定容。

2.2 Ca 同位素化学分离及测定

为了保证 Ca 同位素的回收率及防止化学分离过程中产生的分馏, Ca 样品在上柱前需要加入双稀释剂。取出约 50 μg Ca 样品按比例加入一定量的 ^{42}Ca - ^{43}Ca 双稀释剂混合, 之后将样品加入装有 1mL Bio-rad AG MP-50 (100~200 目) 树脂的 Teflon 离子交换柱中, 并用 1.6 mol/L HCl 淋洗出样品的 Ca 组分。具体化学分离流程及双稀释剂选择参见 (Liu Yufei et al., 2015; Zhu Hongli et al., 2016; Liu Fang et al., 2017)。所有 Ca 同位素样品化学流程回收率控制在~100%, 并且以 IAPSO 大西洋海水及 USGS 标样 BHVO-2 两个国际标样、重复样及空白对化学流程空白进行监控。最终得到的全流程空白为 20~70ng, 相对于 50 μg Ca 的上样量可忽略不计。

Ca 同位素测定是在 Trion TIMS 上完成。取约含 5 μg Ca 的分离好的样品点在 Ta 灯丝带上, 并加入 H_3PO_4 作为激发剂进行测定。Ca 同位素组成的表达方式为 $\delta^{44}\text{Ca} = [(^{44}\text{Ca}/^{40}\text{Ca})_{\text{sample}} / (^{44}\text{Ca}/^{40}\text{Ca})_{\text{SRM 915a}} - 1] \times 1000$, 其中以 NIST SRM 915a 作为参考标准, 并通过 ^{42}Ca - ^{43}Ca 双稀释剂以指数分馏法则进行校正。实验过程中得到的长期 NIST SRM 915a $\delta^{44}\text{Ca} = -0.01 \pm 0.02$ (2SE, $n=37$), IAPSO 大西洋海水 $\delta^{44}\text{Ca} = 1.82 \pm 0.02$ (2SE, $n=20$), USGS 岩石标样 BHVO-2 $\delta^{44}\text{Ca} = 0.76 \pm 0.02$ (2SE, $n=18$), 三种标样的数据均与国际上已发表的参考值在误差范围内一致 (Jochum et al., 2006; Amini et al., 2009; Valdes et al., 2014; Magna et al., 2015; Liu Fang et al., 2017)。

2.3 Mg 同位素化学分离及测定

取出含有 20~50 μg Mg 样品加入到装有 1.25mL Bio-rad AG 50W-X8 (200~400 目) 树脂的离子交换柱中, 并经由 1 mol/L HNO_3 淋洗出来样品的 Mg 组分。由于 Mg 同位素在化学分离过程中存在明显的分馏 (Chang et al., 2003; Teng Fangzhen et al., 2007), 为防止分馏对样品本身 Mg 同位素组分造成影响需要尽可能控制化学分离流程的回收率接近 100%。为此我们将化学分离过程中接取目标元素前后淋洗的溶液同样接取下来, 并通过 ICP-OES 测试其中的 Mg 含量以监控流程

回收率。实验得到的全流程空白为 34~52ng, 不到上样量的 2% 可忽略不计。

Mg 同位素的测定是在 Neptune Plus MC-ICP-MS 上完成, 具体测试流程参见 (An Yajun et al., 2014)。Mg 同位素组成是以 DSM-3 作为参考标准 (Galy et al., 2003), 其表达公式为 $\delta^x\text{Mg} = [(^x\text{Mg}/^{24}\text{Mg})_{\text{sample}} / (^x\text{Mg}/^{24}\text{Mg})_{\text{standard}} - 1] \times 1000$, 其中 x 为 25 或 26。实验测得的国际标样 NIST SRM 980 $\delta^{26}\text{Mg} = -2.82 \pm 0.02$ (2SD, $n=12$)、Cambridge-1 $\delta^{26}\text{Mg} = -2.59 \pm 0.04$ (2SD, $n=15$)、实验室内部标准溶液 IGG-Mg $\delta^{26}\text{Mg} = -1.74 \pm 0.04$ (2SD, $n=22$) 及 USGS 岩石标样 BHVO-2 $\delta^{26}\text{Mg} = -0.25 \pm 0.06$ (2SD, $n=7$), 均与文献值在误差范围一致 (Galy et al., 2003; Pogge Von Strandmann et al., 2008, 2011; Bizzarro et al., 2011; Bouvier et al., 2013; An Yajun et al., 2014; Huang Jian et al., 2015; Huang Kangjun et al., 2015; Teng Fangzhen et al., 2015, 2017)。

3 分析结果

米巴勒和麦嘎地区超钾质岩及选用的国际标样的分析结果见表 1。超钾质岩具有较为均一的 Ca 同位素组成, 其变化范围在 0.59~0.75, 平均值为 0.68 ± 0.04 (2SE, $n=8$), 不仅明显低于上地幔值 $\delta^{44}\text{Ca} = 1.04 \pm 0.05$ (DePaolo, 2004; Amini et al., 2009; Huang Shichun et al., 2010; Simon and DePaolo, 2010), 而且也低于硅酸盐地球值 $\delta^{44}\text{Ca} = 0.94 \pm 0.05$ (Kang Jinting et al., 2017)。

超钾质岩 Mg 同位素组成变化范围为 $-0.33 \sim -0.24$, 平均值为 -0.29 ± 0.03 (2SD, $n=8$), 尽管略低于上地幔 Mg 同位素组成 $\delta^{26}\text{Mg} = -0.25 \pm 0.07$ (Teng Fangzhen et al., 2010), 但仍在误差范围内一致, 表明超钾质岩具有与地幔相近的 Mg 同位素特征。在 $\delta^{25}\text{Mg}$ - $\delta^{26}\text{Mg}$ 图解中 (图 2), 超钾质岩及标样数据均落在了斜率为 0.521 的地球样品平衡质量分馏曲线附近 (Young and Galy, 2004)。

4 讨论

4.1 岩浆演化及风化作用对 Ca-Mg 同位素的影响

岩石的地球化学组成不仅在岩浆演化过程中可能受到部分熔融、分离结晶及地壳混染作用的影响, 也可能在地表环境下受到风化作用影响。因此在通过超钾质岩的 Ca、Mg 同位素特征讨论源区组成前需先排除这些因素对 Ca、Mg 同位素可能造成的干扰。

表 1 米巴勒和麦嘎地区超钾质岩及选用的国际标样 Ca、Mg 同位素分析结果

Table 1 Calcium and magnesium isotopic compositions of ultra-potassic volcanic rocks in Mibale and Maiga areas and reference materials

样品编号	岩石类型	采样位置	$\delta^{44}\text{Ca}$	2SE	$\delta^{25}\text{Mg}$	2SD	$\delta^{26}\text{Mg}$	2SD
CM10-04-08	超钾质岩	米巴勒	0.64	0.05	-0.16	0.03	-0.32	0.03
CM10-04-12	超钾质岩	米巴勒	0.59	0.05	-0.16	0.02	-0.33	0.01
CM10-04-18	超钾质岩	米巴勒	0.70	0.05	-0.16	0.01	-0.33	0.02
CM10-04-20	超钾质岩	米巴勒	0.75	0.05	-0.16	0.03	-0.33	0.03
CM10-04-22	超钾质岩	米巴勒	0.70	0.05	-0.13	0.03	-0.24	0.03
CQQ4-04-01	超钾质岩	麦嘎	0.75	0.05	-0.13	0.02	-0.26	0.02
CQQ4-04-03	超钾质岩	麦嘎	0.66	0.08	-0.15	0.02	-0.28	0.03
CQQ4-04-05	超钾质岩	麦嘎	0.70	0.09	-0.13	0.02	-0.26	0.01
样品编号	标样类型	采样位置	$\delta^{44}\text{Ca}$	2SE	$\delta^{25}\text{Mg}$	2SD	$\delta^{26}\text{Mg}$	2SD
SRM 915a	纯碳酸盐	人工制备	-0.01	0.02				
IAPSO	海水	大西洋	1.82	0.02				
SRM 980	纯 Mg 标液	人工制备			-1.46	0.03	-2.82	0.02
Cambridge-1	纯 Mg 标液	人工制备			-1.34	0.03	-2.59	0.04
IGGMg-1	实验室室内标	人工制备			-0.90	0.02	-1.74	0.04
BHVO-2	玄武岩标样	夏威夷	0.76	0.02	-0.12	0.03	-0.25	0.06

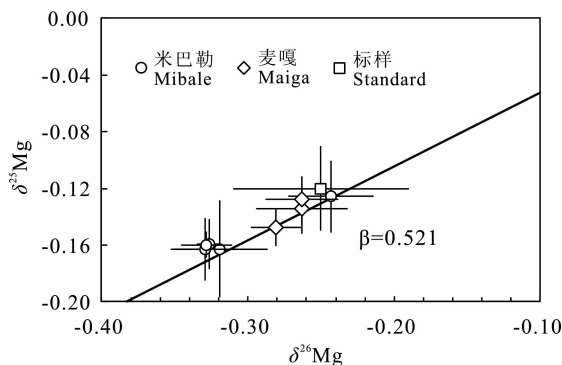
图 2 米巴勒和麦嘎地区超钾质岩及标样的 $\delta^{25}\text{Mg}$ - $\delta^{26}\text{Mg}$ 图解

Fig. 2 Magnesium three-isotope plot of ultra-potassic volcanic rocks from Mibale and Maiga areas and reference material

4.1.1 风化作用

本次研究样品在分析测试前均已经过筛选,只选用新鲜部分进行碎样磨粉。米巴勒和麦嘎地区的超钾质岩显示出较低的 LOI 变化范围(0.49%~3.05%) (表 2),且 CaO、MgO 含量与烧失量无相关性(图 3a,b),表明 Ca、Mg 含量没有受到风化作用的影响。此外,超钾质岩的 $\delta^{44}\text{Ca}$ 、 $\delta^{26}\text{Mg}$ 均没有与 LOI 表现出相关性(图 3c,d)。因此,本文认为超钾质岩的 Ca、Mg 元素含量及同位素组成均未受到风化作用的影响。

4.1.2 地壳混染

目前已有大量的研究结果证明超钾质岩并未受到明显的地壳混染。拉萨地块超钾质岩均具有高 $\text{Mg}^{\#}$ 值、极高的不相容元素含量和含有地幔橄榄

岩、辉石岩等包体等特征,代表其为快速上升的产物,不可能与地壳物质发生反应(Turner et al., 1996; Miller et al., 1999; Williams et al., 2004; Zhao Zhidan et al., 2008; Liu Chuanzhou et al., 2011, 2014; Prelević et al., 2012; Liu Dong et al., 2015)。此外,Huang Feng et al. (2015)对本文研究区域内的超钾质岩样品进行了详细的 Re-Os 同位素研究,指出这些超钾质岩样品均具有高的 MgO 和 Os 含量,并未受到明显的地壳混染。

在岩浆上升过程中,即使少量的地壳混染也能导致岩浆中的铁镁质矿物发生快速结晶及分馏,从而使混染岩浆中的 MgO 、 Fe_2O_3 、 Ni 、 Sc 、 Cr 等含量明显降低,并妨碍 K_2O 富集(Avanzinelli et al., 2009)。样品 CM10-04-18、CM10-04-20 表现出极低的 MgO 含量(<3%)及 $\text{Mg}^{\#}$ 值(42~61),已超出了超钾质岩的定义范围,并且两者的 Fe_2O_3 、微量元素 Ni 、 Cr 也表现出明显较低的含量,同时虽然两者 SiO_2 含量较高(>65%)但它们的 K_2O 含量也没有与之表现出正相关(图 5c),因此这两个样品极可能受到了地壳混染。然而所有超钾质岩样品的 $\delta^{44}\text{Ca}$ 、 $\delta^{26}\text{Mg}$ 值都没有与 $\text{Mg}^{\#}$ 值表现出相关性(图 4a, b),反映出文本研究的超钾质岩样品并未受到明显的地壳混染,与前人的研究结果一致。为了更好地探讨超钾质岩源区的 Ca-Mg 同位素地球化学特征,我们将在后续源区讨论中剔除可能遭受地壳混染影响的两个样品(CM10-04-18 和 CM10-04-20)。

4.1.3 分离结晶及部分熔融

在地幔物质发生部分熔融及后续岩浆结晶分异

表 2 米巴勒和麦嘎地区超钾质岩主量(%)、微量元素($\times 10^{-6}$)数据Table 2 Major (%) and trace element ($\times 10^{-6}$) compositions of ultra-potassic rocks from Mibale and Maiga areas

样品编号	CM10-04-08	CM10-04-12	CM10-04-18	CM10-04-20	CM10-04-22	CQQ4-04-01	CQQ4-04-03	CQQ4-04-05
位置	米巴勒	米巴勒	米巴勒	米巴勒	米巴勒	麦嘎	麦嘎	麦嘎
SiO ₂	55.95	55.99	66.20	65.17	59.10	55.70	54.83	56.00
TiO ₂	1.69	1.56	0.71	0.93	1.62	1.55	1.52	1.46
Al ₂ O ₃	11.04	11.10	14.06	13.41	11.19	11.37	11.45	11.26
TFe ₂ O ₃	5.99	7.53	2.99	3.66	5.04	6.98	7.20	6.27
MnO	0.07	0.08	0.04	0.05	0.06	0.09	0.09	0.08
MgO	7.53	6.96	1.10	2.94	6.35	10.11	10.24	10.66
CaO	5.61	5.84	1.73	2.51	4.13	5.01	5.12	4.14
Na ₂ O	1.56	1.77	2.66	2.48	1.27	1.94	1.58	1.38
K ₂ O	6.63	6.11	7.46	7.68	8.97	6.50	6.74	8.23
P ₂ O ₅	0.55	0.08	0.14	0.04	0.11	0.14	0.19	0.42
LOI	3.05	2.47	2.38	0.74	1.68	0.86	1.20	0.49
Total	99.67	99.49	99.46	99.61	99.52	100.24	100.07	100.37
Mg [#]	71	65	42	61	71	74	74	77
Cr	360.4	449.6	19.46	117.5	366.4	728.9	677.4	592.8
Co	22.68	30.41	7.25	11.92	19.92	18.43	16.76	13.99
Ni	213.3	215.2	15.68	74.24	194.3	305.0	310.2	382.3
Sc	26.93	22.23	13.40	24.90	18.08	21.91	21.03	18.14
V	115.8	146.6	44.30	72.96	123.3	154.7	143.1	125.1
Ga	20.75	18.79	23.90	21.78	21.61	18.32	18.75	19.95
Rb	604.1	504.3	379.4	403.0	590.9	381.3	327.1	635.9
Sr	984.5	1000	667.1	786.2	507.4	1152	1166	684.2
Ba	3881	3626	1722	2065	3695	3737	3661	3888
Nb	52.03	52.66	81.18	53.71	45.07	32.21	30.96	28.83
Ta	2.33	2.98	4.93	3.07	2.68	1.93	1.85	1.61
Zr	885.9	740.5	918.1	663.8	925.1	685.5	660.7	685.0
Hf	20.90	20.54	25.87	18.42	26.66	20.72	19.99	20.55
Y	16.17	12.78	13.88	9.484	12.11	14.73	17.39	17.50
Th	108.4	165.9	234.2	104.9	107.0	201.7	200.8	213.2
U	5.13	16.26	28.91	11.09	2.17	33.84	32.51	34.06
La	123.0	49.65	196.2	113.3	67.98	26.05	34.79	54.70
Ce	269.9	153.4	353.1	210.8	174.2	86.04	111.3	153.0
Pr	35.32	19.60	37.82	24.05	25.20	16.11	20.12	25.56
Nd	128.6	82.07	119.6	80.05	101.3	80.11	100.8	121.9
Sm	18.53	14.62	14.26	10.94	16.26	19.07	22.70	26.11
Eu	2.92	2.37	2.31	2.09	2.42	3.46	3.94	3.68
Gd	8.30	7.66	4.03	4.06	8.05	10.07	12.03	13.78
Tb	0.86	0.83	0.77	0.57	0.83	1.04	1.23	1.31
Dy	3.91	3.67	3.43	2.62	3.56	4.08	4.82	4.75
Ho	0.58	0.57	0.54	0.45	0.53	0.59	0.71	0.68
Er	1.61	1.62	1.59	1.28	1.47	1.48	1.80	1.71
Tm	0.17	0.21	0.19	0.17	0.17	0.19	0.21	0.19
Yb	1.15	1.36	1.31	1.07	1.08	1.18	1.36	1.24
Lu	0.17	0.20	0.19	0.19	0.18	0.17	0.20	0.18

注:米巴勒和麦嘎地区超钾质岩的主量、微量元素数据引自 Chen Jianlin et al., 2012; Huang Feng et al., 2015。

的过程中,由于各元素在不同矿物中的分配系数(D)不同,随着矿物逐渐发生熔融或从熔体中结晶出来,岩浆熔体中的各种元素含量及同位素组成可能发生变化,最终也可能影响岩石的元素含量及同位素组成。

现有研究表明 Mg 同位素在科马提质、玄武质、

花岗质及碱性岩浆结晶分异过程中没有发生明显的同位素分馏,同时在岩浆分异过程中形成的硅酸盐类矿物(如橄榄石、辉石、角闪石或黑云母等)之间也没有明显的 Mg 同位素分馏(Handler et al., 2009; Yang Wei et al., 2009; Young et al., 2009; Dauphas et al., 2010; Liu Shengao et al., 2010,

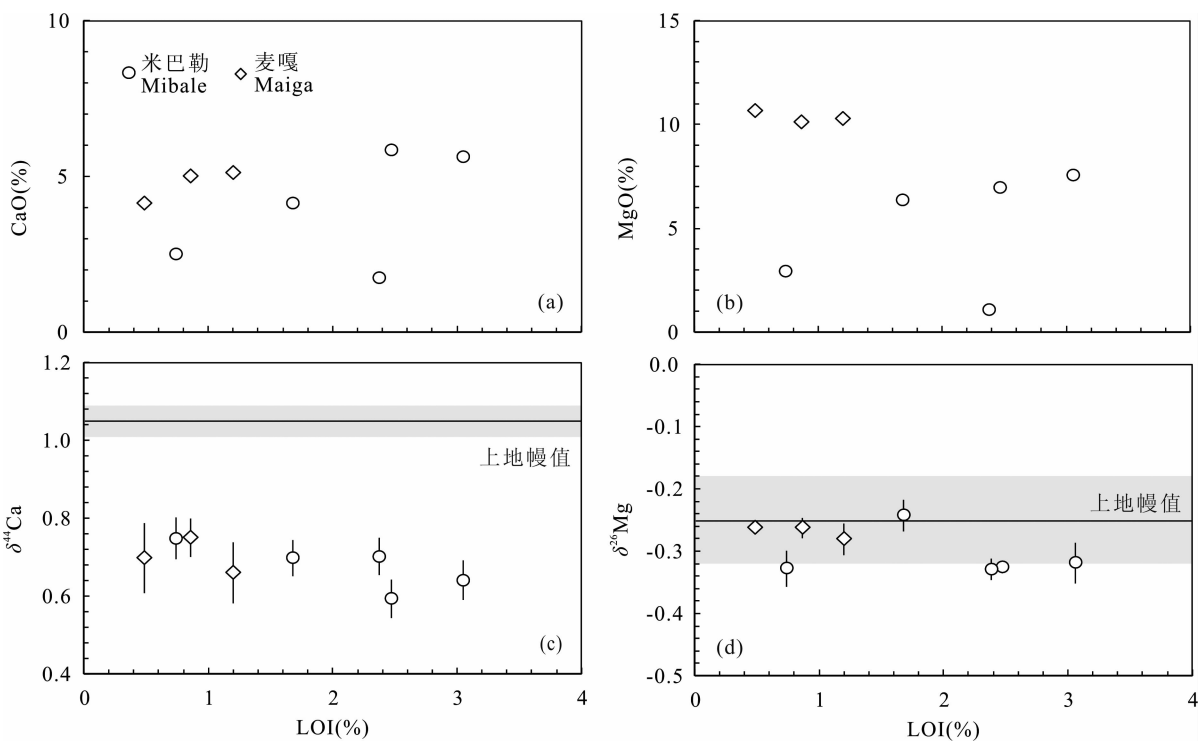


图3 米巴勒和麦嘎地区超钾质岩的 CaO-LOI、MgO-LOI、 $\delta^{44}\text{Ca}$ -LOI 及 $\delta^{26}\text{Mg}$ -LOI 图解

Fig. 3 Plots of LOI content vs. CaO, MgO, $\delta^{44}\text{Ca}$ and $\delta^{26}\text{Mg}$ of ultra-potassic volcanic rocks from Mibale and Maiga areas

$\delta^{44}\text{Ca}$ 和 $\delta^{26}\text{Mg}$ 的地幔值分别引自 Huang Shichun et al., 2010 和 Teng Fangzhen et al., 2010

$\delta^{44}\text{Ca}$ 和 $\delta^{26}\text{Mg}$ values of mantle are from Huang Shichun et al., 2010 and Teng Fangzhen et al., 2010

2011; Pogge Von Strandmann et al., 2011; Xiao Yan et al., 2013; Hu Yan et al., 2016; Ke Shan et al., 2016; Teng Fangzhen, 2017)。但在 Ca 同位素方面, 目前对分离结晶过程中是否存在 Ca 同位素分馏尚没有明确定论, 需要依照样品实际特征进行判断。在哈克图解(图 5a~d)中, 除去可能受地壳混染的样品外, 超钾质岩的 CaO、MgO、 Fe_2O_3 与 SiO_2 呈现出负相关趋势, 表明超钾质岩的形成可能与橄榄石和辉石的结晶分异有关。 SiO_2 含量的高低可以指示岩浆分离结晶程度的大小, 超钾质岩的 Ca、Mg 同位素组成没有与 SiO_2 显示出相关性(图 5e, f), 因此, 超钾质岩的 Ca、Mg 同位素组成没有受到岩浆分离结晶的影响。

另一方面, 在 La/Yb-La 图中超钾质岩表现出正相关趋势(图 6), 且米巴勒地区超钾质岩熔体的 La 含量及 La/Yb 比值均大于麦嘎地区的, 表明两个地区超钾质岩熔体中的元素变化都是受部分熔融控制。若两者均来源于同一地幔源区, 则米巴勒超钾质岩的源区比麦嘎超钾质岩源区的部分熔融程度更低。已有研究指出不同程度的部分熔融可能导致熔体的 Ca 同位素产生分馏(Amini et al., 2009;

Huang Shichun et al., 2010; Simon and DePaolo, 2010), 但米巴勒和麦嘎地区的超钾质岩 $\delta^{44}\text{Ca}$ 、 $\delta^{26}\text{Mg}$ 值均没有与 Sm/Yb、Nb/Y 值显示出相关性(图 4c~f), 这就指示出超钾质岩的 Ca、Mg 同位素组成没有受到部分熔融的影响。

综上所述, 地表风化、地壳混染、结晶分离及部分熔融等作用均没有对超钾质岩 Ca、Mg 同位素组成产生影响。因此, 本文研究的超钾质岩 Ca、Mg 同位素组成可以代表其地幔源区形成的原始岩浆的同位素组成。

4.2 超钾质岩 Ca 同位素特征

Gausonne et al. (2016) 在前人研究的基础上总结了目前已发表的所有岩浆岩的 Ca 同位素数据, 发现尽管不同类型的岩浆岩 $\delta^{44}\text{Ca}$ 值具有较大的变化范围(0.6~1.6), 但大部分岩浆岩具有较一致的分布范围, 其 $\delta^{44}\text{Ca}$ 平均值为 0.80 ± 0.10 。米巴勒和麦嘎地区的超钾质岩 $\delta^{44}\text{Ca}$ 值为 $0.59 \sim 0.78$, 平均值为 0.69 ± 0.02 ($2\text{SE}, n=8$)。其 Ca 同位素组成不仅明显低于上地幔值($\delta^{44}\text{Ca} = 1.05 \pm 0.04$, Huang Shichun et al., 2010)及硅酸盐地球值($\delta^{44}\text{Ca} = 0.94 \pm 0.05$, Kang Jinting et al., 2017),

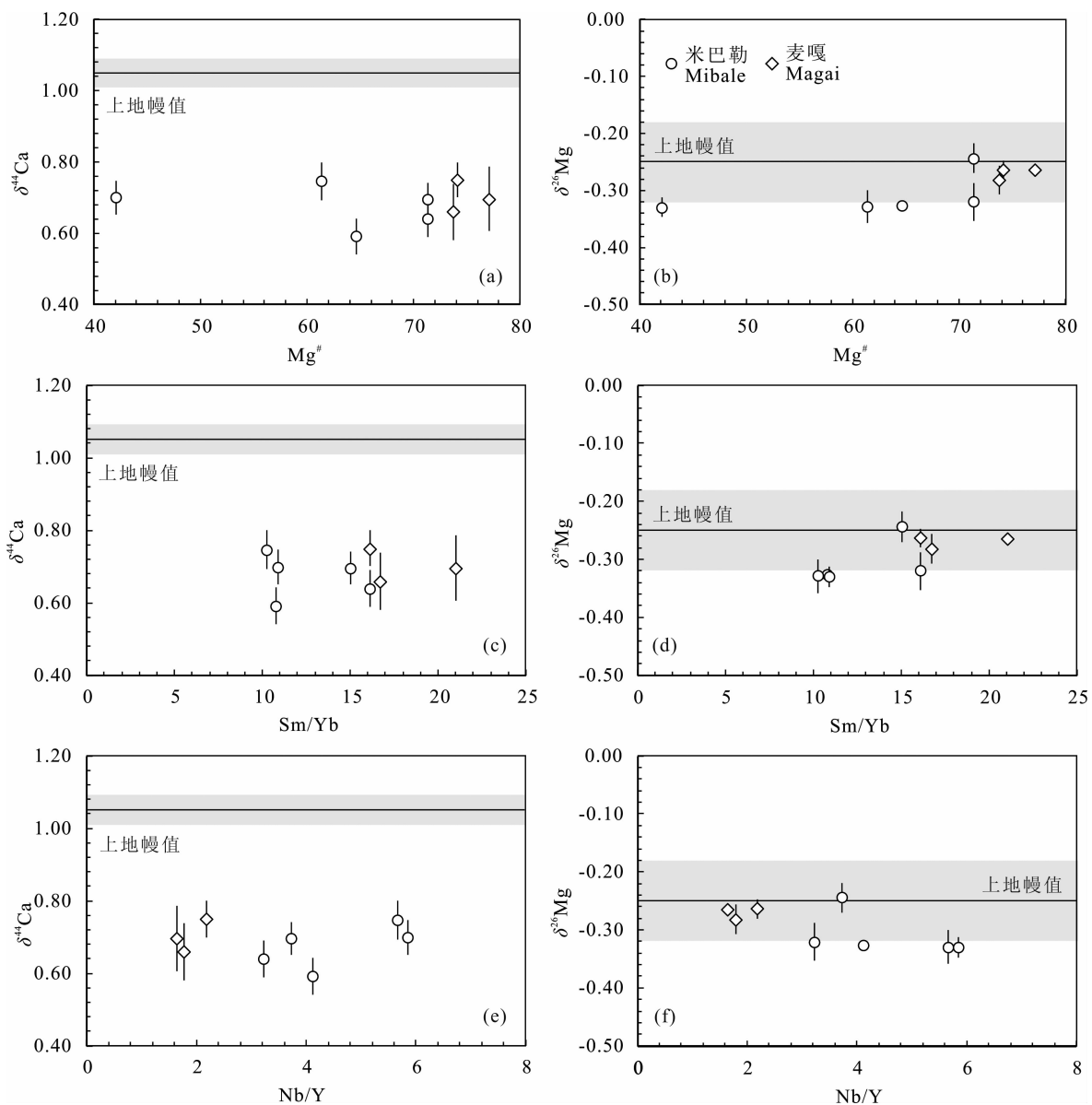


图 4 米巴勒和麦嘎地区超钾质岩 $\delta^{44}\text{Ca}$ 、 $\delta^{26}\text{Mg}$ vs. $\text{Mg}^{\#}$ ， $\delta^{44}\text{Ca}$ 、 $\delta^{26}\text{Mg}$ vs. Sm/Yb ， $\delta^{44}\text{Ca}$ 、 $\delta^{26}\text{Mg}$ vs. Nb/Y 图解

Fig. 4 Plots of $\delta^{44}\text{Ca}$, $\delta^{26}\text{Mg}$ vs. $\text{Mg}^{\#}$, Sm/Yb and Nb/Y of ultra-potassic volcanic rocks from Mibale and Maiga areas

$\delta^{44}\text{Ca}$ 和 $\delta^{26}\text{Mg}$ 的地幔值分别引自 Huang Shichun et al., 2010 和 Teng Fangzhen et al., 2010

$\delta^{44}\text{Ca}$ and $\delta^{26}\text{Mg}$ values of mantle are from Huang Shichun et al., 2010 and Teng Fangzhen et al., 2010

也比大部分已发表岩浆岩的 $\delta^{44}\text{Ca}$ 值低(图 7)。因此,拉萨地块超钾质岩的富集地幔源区具有较低的 $\delta^{44}\text{Ca}$ 值。然而,已有的数据显示地幔物质具有本文超钾质岩明显不同的 Ca 同位素组成,表明可能有低 Ca 同位素组成的物质加入到地幔交代形成了超钾质岩石的特殊地幔源区特征。

目前关于超钾质岩富集地幔源区组成的观点中,加入地幔的物质既可能是俯冲的印度大陆地壳物质,也可能是陆陆碰撞前俯冲的新特提斯洋壳沉积物。不同来源的物质,加入地幔源区后会对 Ca 同位素组成造成不同的影响。已有研究表明超钾质

岩地幔源区是交代作用的产物,交代物质必定比地幔物质所占比例要小得多。因此,无论源区 Ca 同位素组成如何变化,其变化范围都应在交代物质与上地幔的 Ca 同位素组成之间并接近地幔端元。超钾质岩的 $\delta^{44}\text{Ca}$ 值表现出明显低于上地幔值的特征,其源区交代物质的 $\delta^{44}\text{Ca}$ 值必定比超钾质岩的 $\delta^{44}\text{Ca}$ 值更低,目前已探明的地球储库中只有海相碳酸盐具有极低的 $\delta^{44}\text{Ca}$ 值(图 7),一些古老海相碳酸盐沉积物 $\delta^{44}\text{Ca}$ 值甚至能低于 0.2 (Huang Shichun et al., 2011),因此超钾质岩源区交代上地幔的物质极可能是海相碳酸盐沉积物。

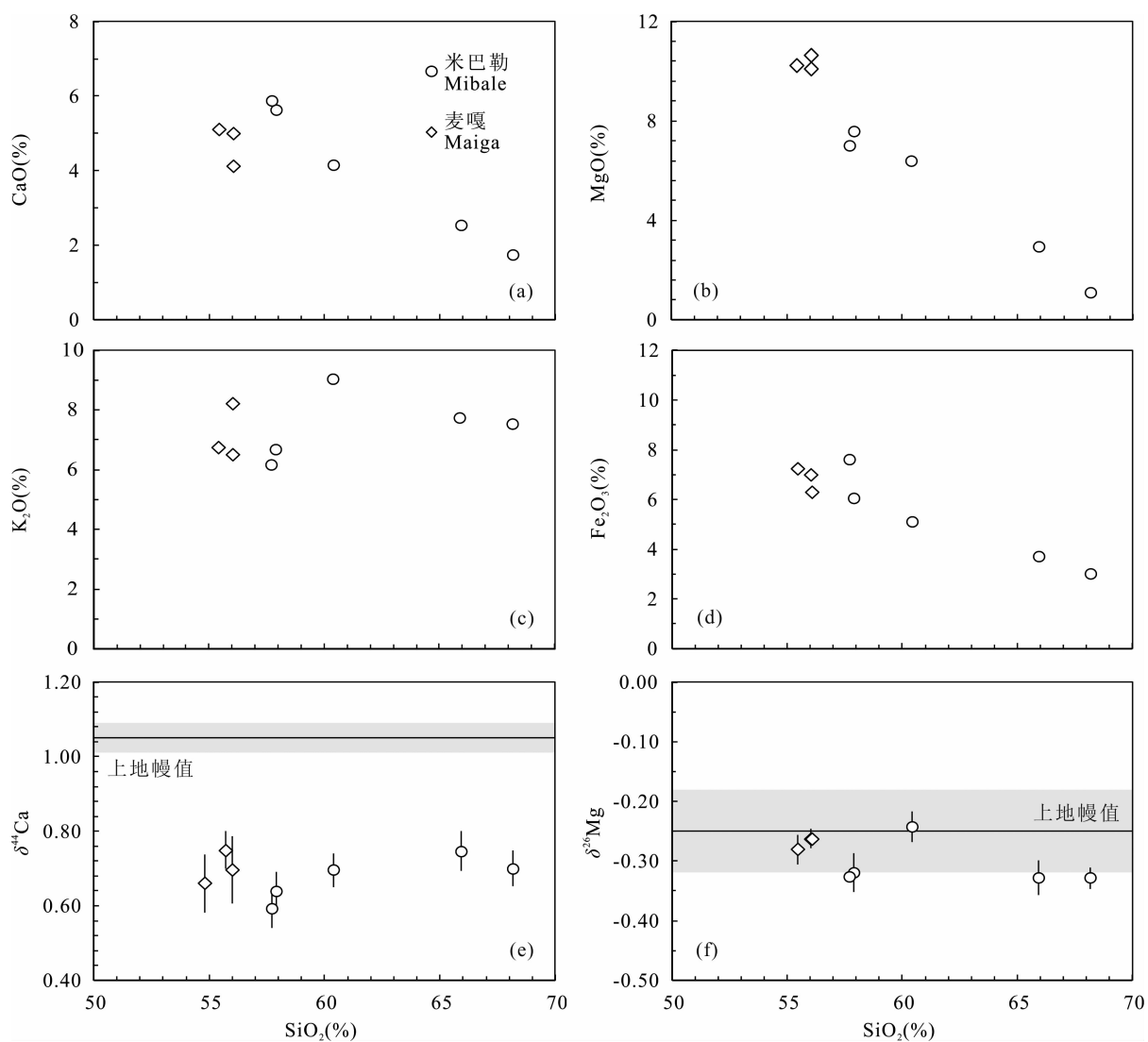
图 5 米巴勒和麦嘎地区超钾质岩哈克图解和 $\delta^{44}\text{Ca}$ -SiO₂, $\delta^{26}\text{Mg}$ -SiO₂ 图解

Fig. 5 Harker Plots and plots of SiO₂ contents vs. $\delta^{44}\text{Ca}$, $\delta^{26}\text{Mg}$ of ultra-potassic volcanic rocks from Mibale and Maiga areas

$\delta^{44}\text{Ca}$ 和 $\delta^{26}\text{Mg}$ 的地幔值分别引自 Huang Shichun et al., 2010 和 Teng Fangzhen et al., 2010

$\delta^{44}\text{Ca}$ and $\delta^{26}\text{Mg}$ values of mantle are from Huang Shichun et al., 2010 and Teng Fangzhen et al., 2010

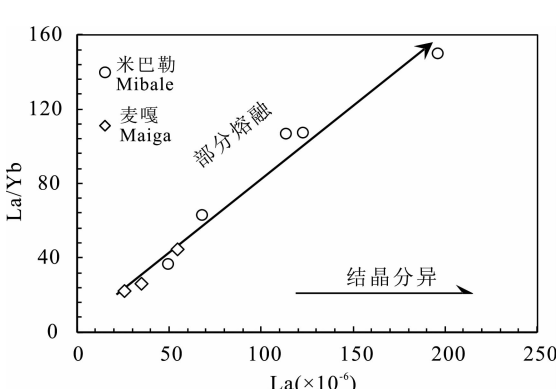


图 6 米巴勒和麦嘎地区超钾质岩 La/Yb-La 图解

Fig. 6 Plot of La/Yb vs. La of ultra-potassic volcanic rocks from Mibale and Maiga areas

4.3 超钾质岩 Mg 同位素特征

尽管米巴勒和麦嘎地区超钾质岩的 $\delta^{44}\text{Ca}$ 值表现出明显低于上地幔值的特征,但其 $\delta^{26}\text{Mg}$ 值变化范围为 $-0.33 \sim -0.24$ (平均值为 -0.29 ± 0.03 , 2SD, $n=8$),与上地幔的 Mg 同位素组成在误差范围内一致。米巴勒和麦嘎地区的超钾质岩均来源于富集地幔,其与上地幔相近的 Mg 同位素组成很可能继承了地幔原有的 Mg 同位素特征的结果。尽管交代作用形成了超钾质岩的富集地幔源区,但地球上绝大部分 Mg 都储存在地幔中(>99%),即使交代物质的 Mg 同位素组成与地幔有所差异,其相对地幔极少的 Mg 含量(相差两个数量级以上)很难对地幔中的 Mg 同位素组成产生明显变化。此外,

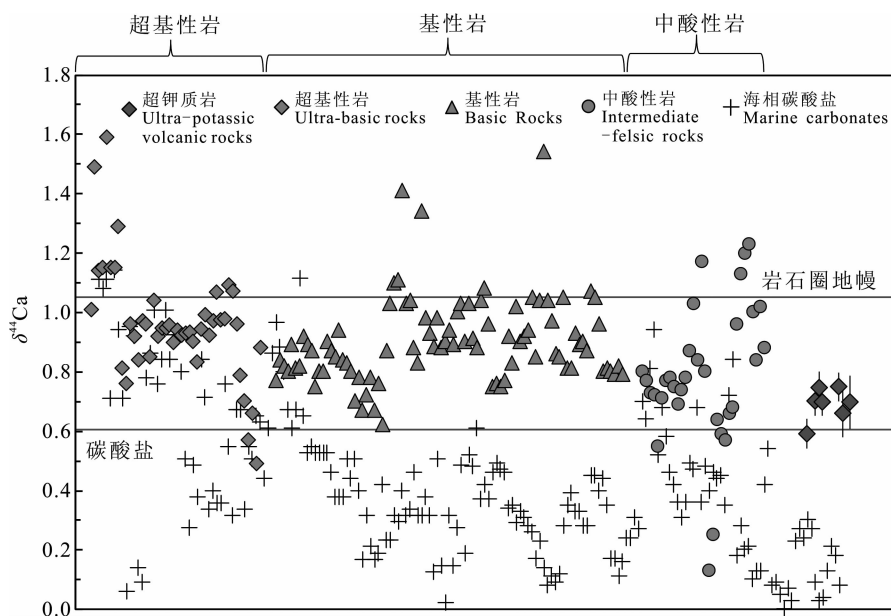
图 7 岩浆岩、海相碳酸盐及超钾质岩 $\delta^{44}\text{Ca}$ 图解

Fig. 7 Plot of Ca isotopic compositions of igneous rocks, marine carbonates and ultra-potassic volcanic rocks

数据来源: Skulan et al., 1997; Richter et al., 2003; DePaolo, 2004; Immenhauser et al., 2005; Steuber and Buhl, 2006; Farkas et al., 2007; Amini et al., 2009; Holmden and Belanger, 2010; Huang Shichun et al., 2010, 2011; Payne et al., 2010; Simon and DePaolo, 2010; John et al., 2012; Schiller et al., 2012; Colla et al., 2013; Hindshaw et al., 2013; Valdes et al., 2014; Jacobson et al., 2015; Magna et al., 2015; Kang Jinting et al., 2016, 2017; Liu Fang et al., 2017

Data are from Skulan et al., 1997; Richter et al., 2003; DePaolo, 2004; Immenhauser et al., 2005; Steuber and Buhl, 2006; Farkas et al., 2007; Amini et al., 2009; Holmden and Belanger, 2010; Huang Shichun et al., 2010, 2011; Payne et al., 2010; Simon and DePaolo, 2010; John et al., 2012; Schiller et al., 2012; Colla et al., 2013; Hindshaw et al., 2013; Valdes et al., 2014; Jacobson et al., 2015; Magna et al., 2015; Kang Jinting et al., 2016, 2017; Liu Fang et al., 2017

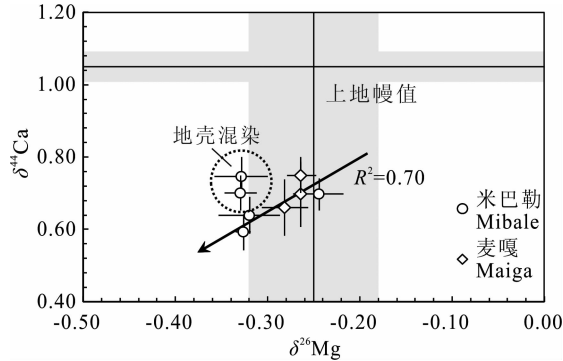
图 8 米巴勒和麦嘎地区超钾质岩 $\delta^{44}\text{Ca}$ - $\delta^{26}\text{Mg}$ 图解

Fig. 8 Plot of $\delta^{44}\text{Ca}$ vs. $\delta^{26}\text{Mg}$ of ultra-potassic

volcanic rocks form Mibale and Maiga areas

$\delta^{44}\text{Ca}$ 和 $\delta^{26}\text{Mg}$ 的地幔值分别引自 Huang Shichun et al., 2010

和 Teng Fangzhen et al., 2010

$\delta^{44}\text{Ca}$ and $\delta^{26}\text{Mg}$ values of mantle are from Huang Shichun et al.,

2010 and Teng Fangzhen et al., 2010

在排除可能受到地壳混染的样品后, 超钾质岩的 Ca、Mg 同位素之间表现出一定的正相关性(图 8), 随着 $\delta^{44}\text{Ca}$ 值的减小, 超钾质岩的 $\delta^{26}\text{Mg}$ 值也表现出减小趋势。拉萨地块内超钾质岩的地幔源区可能

具有低 Ca 同位素组成的物质加入, 因此, 交代物质端元应同时具有低 $\delta^{44}\text{Ca}$ 、低 $\delta^{26}\text{Mg}$ 值的特征。俯冲的新特提斯洋壳碳酸盐沉积物同时具有低 Ca、Mg 同位素特征, 因此, 我们认为超钾质岩很可能有来自俯冲新特提斯洋壳的碳酸盐沉积物加入改造的地幔源区。

5 结论

(1) 米巴勒、麦嘎超钾质岩的 Ca、Mg 同位素组成没有受到地表风化作用及岩浆后期作用的影响, 可直接指示其地幔源区的特征。

(2) 米巴勒、麦嘎超钾质岩的 Ca 同位素组成 $\delta^{44}\text{Ca}$ 值为 0.59~0.75, 明显低于上地幔、硅酸盐地球及其他已发表岩浆岩的 Ca 同位素组成, 表明其源区很可能加入了俯冲新特提斯洋壳的碳酸盐沉积物。

(3) 米巴勒、麦嘎超钾质岩的 Mg 同位素组成 $\delta^{26}\text{Mg}$ 值为 -0.33~-0.24, 表现出与上地幔 $\delta^{26}\text{Mg}$ 值相近的特征。同时超钾质岩的 Mg-Ca 同位素之

间存在正相关性,指示其源区应有同时具有低Ca、低Mg同位素组成的物质加入,进一步证明其很可能来自俯冲新特提斯洋壳的碳酸盐沉积物。

致谢:感谢中国科学院广州地球化学研究所马金龙、孙胜玲及刘颖在实验过程中提供的支持与帮助,感谢各位审稿人在文章审稿过程提出的宝贵意见。

References

- Amini M, Eisenhauer A, Böhm F, Holmden C, Kreissig K, Hauff F, Jochum K P. 2009. Calcium isotopes ($\delta^{44/40}$ Ca) in MPI-DING reference glasses, USGS rock powders and various rocks: Evidence for Ca isotope fractionation in terrestrial silicates. *Geostandards and Geoanalytical Research*, 33(2): 231~247.
- An Yajun, Wu Fei, Xiang Yuanxin, Nan Xiaoyun, Yu Xun, Yang Jinhui, Yu Huimin, Xie Liewen, Huang Fang. 2014. High-precision Mg isotope analyses of low-Mg rocks by MC-ICP-MS. *Chemical Geology*, 390: 9~21.
- Avanzinelli R, Lustrino M, Mattei M, Melluso L, Conticelli S. 2009. Potassic and ultrapotassic magmatism in the circum-Tyrrhenian region: Significance of carbonated pelitic vs. pelitic sediment recycling at destructive plate margins. *Lithos*, 113(1): 213~227.
- Bizzarro M, Paton C, Larsen K, Schiller M, Trinquier A, Ulfbeck D. 2011. High-precision Mg-isotope measurements of terrestrial and extraterrestrial material by HR-MC-ICP-MS—implications for the relative and absolute Mg-isotope composition of the bulk silicate Earth. *Journal of Analytical Atomic Spectrometry*, 26(3): 565~577.
- Bouvier A, Wadhwa M, Simon S B, Grossman L. 2013. Magnesium isotopic fractionation in chondrules from the Murchison and Murray CM2 carbonaceous chondrites. *Meteoritics & Planetary Science*, 48(3): 339~353.
- Chang V T C, Makishima A, Belshaw N S, O'Nions R K. 2003. Purification of Mg from low-Mg biogenic carbonates for isotope ratio determination using multiple collector ICP-MS. *Journal of Analytical Atomic Spectrometry*, 18(4): 296~301.
- Chen Jianlin, Xu Jifeng, Kang Zhiqiang, Wang Baodi. 2007. Geochemistry and origin of Miocene volcanic rocks in Cazé area, south-western Qinghai-Xizang plateau. *Geochimica*, 36(05): 437~447 (in Chinese with English abstract).
- Chen Jianlin, Xu Jifeng, Kang Zhiqiang, Wang Baodi. 2008. Geochemical comparison of the Cenozoic high-MgO-potassic volcanic rocks between northern and southern of Tibetan Plateau: difference of the both mantle sources. *Acta Petrologica Sinica*, 24(02): 211~224 (in Chinese with English abstract).
- Chen Jianlin, Xu Jifeng, Wang Baodi, Kang Zhiqiang, Jie Li. 2010. Origin of Cenozoic alkaline potassic volcanic rocks at Konglongxiang, Lhasa terrane, Tibetan Plateau: Products of partial melting of a mafic lower-crustal source? *Chemical Geology*, 273(3~4): 286~299.
- Chen Jianlin, Xu Jifeng, Wang Baodi, Kang Zhiqiang. 2012. Cenozoic Mg-rich potassic rocks in the Tibetan Plateau: Geochemical variations, heterogeneity of subcontinental lithospheric mantle and tectonic implications. *Journal of Asian Earth Sciences*, 53: 115~130.
- Colla C A, Wimpenny J, Yin Qingzhu, Rustad J R, Casey W H. 2013. Calcium-isotope fractionation between solution and solids with six, seven or eight oxygens bound to Ca(II). *Geochimica et Cosmochimica Acta*, 121(15): 363~373.
- Dauphas N, Teng Fangzhen, Arndt N T. 2010. Magnesium and iron isotopes in 2.7 Ga Alexo komatiites: mantle signatures, no evidence for Soret diffusion, and identification of diffusive transport in zoned olivine. *Geochimica et Cosmochimica Acta*, 74(11): 3274~3291.
- Depaolo D J. 2004. Calcium isotopic variations produced by biological, kinetic, radiogenic and nucleosynthetic processes. *Reviews in Mineralogy and Geochemistry*, 55(1): 255~288.
- Dewey J F, Shackleton R M, Chang Chengfa, Sun Yiyin. 1988. The tectonic evolution of the Tibetan Plateau. *Philosophical Transactions of the Royal Society of London A: Mathematical, Physical and Engineering Sciences*, 327(1594): 379~413.
- Ding Lin, Kapp P, Zhong Dalai, Deng Wanming. 2003. Cenozoic volcanism in Tibet: Evidence for a transition from oceanic to continental subduction. *Journal of Petrology*, 44(10): 1833~1865.
- Ding Lin, Yue Yahui, Cai Fulong, Xu Xiaoxia, Zhang Qinghai, Lai Qingzhou. 2006. $^{40}\text{Ar}/^{39}\text{Ar}$ Geochronology, geochemical and Sr-Nd-O isotopic characteristics of the high-Mg ultrapotassic rocks in Lhasa block of Tibet: Implications in the onset time and depth of NS-striking rift system. *Acta Geologica Sinica*, 80(09): 1252~1261 (in Chinese with English abstract).
- Farkas J, Boehm F, Wallmann K, Blenkinsop J, Eisenhauer A, van Geldern R, Munnecke A, Voigt S, Veizer J. 2007. Calcium isotope record of Phanerozoic oceans: Implications for chemical evolution of seawater and its causative mechanisms. *Geochimica et Cosmochimica Acta*, 71(21): 5117~5134.
- Galy A, Yoffe O, Janney P E, Williams R W, Cloquet C, Alard O, Halicz L, Wadhwa M, Hutcheon I D, Ramon E, Carignan J. 2003. Magnesium isotope heterogeneity of the isotopic standard SRM980 and new reference materials for magnesium-isotope-ratio measurements. *Journal of Analytical Atomic Spectrometry*, 18(11): 1352.
- Gao Yongfeng, Hou Zengqian, Kamber B S, Wei Ruihua, Meng Xiangjin, Zhao Rongsheng. 2007. Lamproitic rocks from a continental collision zone: evidence for recycling of subducted Tethyan oceanic sediments in the mantle beneath southern Tibet. *Journal of Petrology*, 48(4): 729~752.
- Gausonne N, Schmitt A D, Heuser A, Wombacher F, Dietzel M, Tipper E, Schiller M. 2016. Calcium stable isotope

- geochemistry. Berlin Heidelberg: Springer, 223~244.
- Guo Zhengfu, Wilson M, Zhang Maoliang, Cheng Zhihui, Zhang Lihong. 2013. Post-collisional, K-rich mafic magmatism in south Tibet: Constraints on Indian slab-to-wedge transport processes and plateau uplift. *Contributions to Mineralogy and Petrology*, 165(6): 1311~1340.
- Guo Zhengfu, Wilson M, Zhang Maoliang, Cheng Zhihui, Zhang Lihong. 2015. Post-collisional ultrapotassic mafic magmatism in South Tibet: Products of partial melting of pyroxenite in the mantle wedge induced by roll-back and delamination of the subducted Indian continental lithosphere slab. *Journal of Petrology*, 56(7): 1365~1406.
- Handler M R, Baker J A, Schiller M, Bennett V C, Yaxley G M. 2009. Magnesium stable isotope composition of Earth's upper mantle. *Earth and Planetary Science Letters*, 282(1): 306~313.
- Hébert R, Guilmette C, Dostal J, Bezard R, Lesage G, Bédard é, Wang Chengshan. 2014. Miocene post-collisional shoshonites and their crustal xenoliths, Yarlung Zangbo Suture Zone southern Tibet: Geodynamic implications. *Gondwana Research*, 25(3): 1263~1271.
- Hindshaw R S, Bourdon B, Pogge Von Strandmann P A E P, Vigier N, Burton K W. 2013. The stable calcium isotopic composition of rivers draining basaltic catchments in Iceland. *Earth & Planetary Sciences Letters*, 374(374): 173~184.
- Holmden C, Belanger N. 2010. Ca isotope cycling in a forested ecosystem. *Geochimica et Cosmochimica Acta*, 74(3): 995~1015.
- Hu Yan, Teng Fangzhen, Plank T, Huang Kangjun. 2017. Magnesium isotopic composition of subducting marine sediments. *Chemical Geology*, 466: 15~31.
- Hu Yan, Teng Fangzhen, Zhang Hongfu, Xiao Yan, Su Benxun. 2016. Metasomatism-induced mantle magnesium isotopic heterogeneity: Evidence from pyroxenites. *Geochimica et Cosmochimica Acta*, 185: 88~111.
- Huang Feng, Chen Jianlin, Xu Jifeng, Wang Baodi, Li Jie. 2015. Os-Nd-Sr isotopes in Miocene ultrapotassic rocks of southern Tibet: Partial melting of a pyroxenite-bearing lithospheric mantle? *Geochimica et Cosmochimica Acta*, 163: 279~298.
- Huang Jian, Li Shuguang, Xiao Yilin, Ke Shan, Li Wangye, Tian Ye. 2015. Origin of low $\delta^{26}\text{Mg}$ Cenozoic basalts from South China Block and their geodynamic implications. *Geochimica et Cosmochimica Acta*, 164: 298~317.
- Huang Kangjun, Shen Bing, Lang Xianguo, Tang Wenbo, Peng Yang, Ke Shan, Kaufman A J, Ma Haoran, Li Fangbing. 2015. Magnesium isotopic compositions of the Mesoproterozoic dolostones: Implications for Mg isotopic systematics of marine carbonates. *Geochimica et Cosmochimica Acta*, 164: 333~351.
- Huang Shichun, Farkas J, Jacobsen S B. 2011. Stable calcium isotopic compositions of Hawaiian shield lavas: Evidence for recycling of ancient marine carbonates into the mantle. *Geochimica et Cosmochimica Acta*, 75(17): 4987~4997.
- Huang Shichun, Farkas J, Jacobsen S B. 2010. Calcium isotopic fractionation between clinopyroxene and orthopyroxene from mantle peridotites. *Earth and Planetary Science Letters*, 292(3/4): 337~344.
- Immenhauser A, Nägler T F, Steuber T, Hippler D. 2005. A critical assessment of mollusk $^{18}\text{O}/^{16}\text{O}$, Mg/Ca, and $^{44}\text{Ca}/^{40}\text{Ca}$ ratios as proxies for Cretaceous seawater temperature seasonality. *Palaeogeography, Palaeoclimatology, Palaeoecology*, 215(3): 221~237.
- Jacobson A D, Andrews M G, Lehn G O, Holmden C. 2015. Silicate versus carbonate weathering in Iceland: New insights from Ca isotopes. *Earth & Planetary Science Letters*, 416: 132~142.
- Jochum K P, Stoll B, Herwig K, Willbold M, Hofmann A W, Amini M, Aarburg S, Abouchami W, Hellebrand E, Mocek B. 2006. MPI-DING reference glasses for in situ microanalysis: New reference values for element concentrations and isotope ratios. *Geochemistry, Geophysics, Geosystems*, 7(2): 1525~2027.
- John T, Gussone N, Podladchikov Y Y, Bebout G E, Dohmen R, Halama R, Klemd R, Magna T, Seitz H M. 2012. Volcanic arcs fed by rapid pulsed fluid flow through subducting slabs. *Nature Geoscience*, 5(7): 489~492.
- Kang Jinting, Ionov D A, Liu Fang, Zhang Chenlei, Golovin A V, Qin Liping, Zhang Zhaofeng, Huang Fang. 2017. Calcium isotopic fractionation in mantle peridotites by melting and metasomatism and Ca isotope composition of the Bulk Silicate Earth. *Earth and Planetary Science Letters*, 474: 128~137.
- Kang Jinting, Zhu Hongli, Liu Yufei, Liu Fang, Wu Fei, Hao Yantao, Zhi Xiachen, Zhang Zhaofeng, Huang Fang. 2016. Calcium isotopic composition of mantle xenoliths and minerals from Eastern China. *Geochimica et Cosmochimica Acta*, 174: 335~344.
- Ke Shan, Teng Fangzhen, Li Shuguang, Gao Ting, Liu Shengao, He Yongsheng, Mo Xuanxue. 2016. Mg, Sr, and O isotope geochemistry of syenites from northwest Xinjiang, China: Tracing carbonate recycling during Tethyan oceanic subduction. *Chemical Geology*, 437: 109~119.
- Liao Siping, Chen Zhenhua, Luo Xiaochuan, Zou Aijian. 2002. Discovery of leucite phonolite in the Tangra Yumco area, Tibet and its geological significance. *Geological Bulletin of China*, 21(11): 735~738 (in Chinese with English abstract).
- Liu Chuanzhou, Wu Fuyuan, Chung Sunlin, Li Qiuli, Sun Weidong, Ji Weiqiang. 2014. A 'hidden' ^{18}O -enriched reservoir in the sub-arc mantle. *Scientific Reports*, 4: 4232.
- Liu Chuanzhou, Wu Fuyuan, Chung Sunlin, Zhao Zhidan. 2011. Fragments of hot and metasomatized mantle lithosphere in Middle Miocene ultrapotassic lavas, southern Tibet. *Geology*, 39(10): 923~926.
- Liu Dong, Zhao Zhidan, Zhu Dicheng, Niu Yaoling, Depaolo D J, Harrison T M, Mo Xuanxue, Dong Guochen, Zhou Su, Sun

- Chenguang, Zhang Zhaochong, Liu Junlai. 2014a. Postcollisional potassic and ultrapotassic rocks in southern Tibet: Mantle and crustal origins in response to India-Asia collision and convergence. *Geochimica et Cosmochimica Acta*, 143: 207~231.
- Liu Dong, Zhao Zhidan, Zhu Dichen, Niu Yaoling, Harrison T M. 2014b. Zircon xenocrysts in Tibetan ultrapotassic magmas: Imaging the deep crust through time. *Geology*, 42(1): 43~46.
- Liu Dong, Zhao Zhidan, Zhu Dichen, Niu Yaoling, Widom E, Teng Fangzhen, Depaolo D J, Ke Shan, Xu Jifeng, Wang Qing. 2015. Identifying mantle carbonatite metasomatism through Os-Sr-Mg isotopes in Tibetan ultrapotassic rocks. *Earth and Planetary Science Letters*, 430: 458~469.
- Liu Fang, Zhu Hongli, Li Xin, Wang Guiqin, Zhang Zhaofeng. 2017. Calcium isotopic fractionation and compositions of geochemical reference materials. *Geostandards and Geoanalytical Research*, 41(04): 675~688.
- Liu Pingping, Teng Fangzhen, Dick H J B, Zhou Meifu, Chung Sunlin. 2017. Magnesium isotopic composition of the oceanic mantle and oceanic Mg cycling. *Geochimica et Cosmochimica Acta*, 206: 151~165.
- Liu Shengao, Teng Fangzhen, He Yongsheng, Ke Shan, Li Shuguang. 2010. Investigation of magnesium isotope fractionation during granite differentiation: Implication for Mg isotopic composition of the continental crust. *Earth and Planetary Science Letters*, 297(3): 646~654.
- Liu Shengao, Teng Fangzhen, Yang Wei, Wu Fuyuan. 2011. High-temperature inter-mineral magnesium isotope fractionation in mantle xenoliths from the North China craton. *Earth and Planetary Science Letters*, 308(1): 131~140.
- Liu Yufei, Zhu Hongli, Liu Fang, Wang Guiqin, Xu Jifeng, Zhang Zhaofeng. 2015. Methodological study of chemical separation of calcium for TIMS measurements. *Geochimica*, 44(05): 469~476 (in Chinese with English abstract).
- Magna T, Gussone N, Mezger K. 2015. The calcium isotope systematics of Mars. *Earth & Planetary Science Letters*, 430: 86~94.
- Miller C, Schuster R, Klötzli U, Frank W, Purtscheller F. 1999. Post-Collisional Potassic and ultrapotassic magmatism in SW Tibet: Geochemical and Sr-Nd-Pb-O isotopic constraints for mantle source characteristics and petrogenesis. *Journal of Petrology*, 40(9): 699~715.
- Payne J L, Turchyn A V, Paytan A, Depaolo D J, Lehrmann D J, Yu Meiyi, Wei Jiayong. 2010. Calcium isotope constraints on the end-Permian mass extinction. *Proceedings of the National Academy of Sciences of the United States of America*, 107(19): 8543~8548.
- Pogge Von Strandmann P A E P, Burton K W, James R H, van Calsteren P, Gislason S R, Sigfusson B. 2008. The influence of weathering processes on riverine magnesium isotopes in a basaltic terrain. *Earth and Planetary Science Letters*, 276(1): 187~197.
- Pogge Von Strandmann P A E P, Elliott T, Marschall H R, Coath C, Lai Yijen, Jeffcoate A B, Ionov D A. 2011. Variations of Li and Mg isotope ratios in bulk chondrites and mantle xenoliths. *Geochimica et Cosmochimica Acta*, 75(18): 5247~5268.
- Prelević D, Akal C, Foley S F, Romer R L, Stracke A, Van Den Bogaard P. 2012. Ultrapotassific rocks as geochemical proxies for post-collisional dynamics of orogenic lithospheric mantle: the case of southwestern Anatolia, Turkey. *Journal of Petrology*, 53(5): 1019~1055.
- Richter F M, Davis A M, Depaolo D J, Watson E B. 2003. Isotope fractionation by chemical diffusion between molten basalt and rhyolite. *Geochimica et Cosmochimica Acta*, 67(20): 3905~3923.
- Schiller M, Paton C, Bizzarro M. 2012. Calcium isotope measurement by combined HR-MC-ICP-MS and TIMS. *Journal of Analytical Atomic Spectrometry*, 27(1): 38~49.
- Simon J I, Depaolo D J. 2010. Stable calcium isotopic composition of meteorites and rocky planets. *Earth and Planetary Science Letters*, 289(3): 457~466.
- Skulan J, Depaolo D J, Owens T L. 1997. Biological control of calcium isotopic abundances in the global calcium cycle. *Geochimica et Cosmochimica Acta*, 61(12): 2505~2510.
- Steuber T, Buhl D. 2006. Calcium-isotope fractionation in selected modern and ancient marine carbonates. *Geochimica et Cosmochimica Acta*, 70(22): 5507~5521.
- Su Benxun, Hu Yan, Teng Fangzhen, Xiao Yan, Zhou Xinhua, Sun Yang, Zhou Meifu, Chang Suchin. 2017. Magnesium isotope constraints on subduction contribution to Mesozoic and Cenozoic East Asian continental basalts. *Chemical Geology*, 466: 116~122.
- Sun Chenguang, Zhao Zhidan, Mo Xuanxue, Zhu Dichen, Dong Guochen, Zhou Su, Dong Xin, Xie Guogang. 2007. Geochemistry and origin of the Miocene Sailipu ultrapotassic rocks in western Lhasa block, Tibetan Plateau. *Acta Petrologica Sinica*, 23(11): 2715~2726 (in Chinese with English abstract).
- Sun Chenguang, Zhao Zhidan, Mo Xuanxue, Zhu Dichen, Dong Guochen, Zhou Su, Chen Haihong, Xie Liwen, Yang Yueheng, Sun Jinfeng, Yu Feng. 2008. Enriched mantle source and petrogenesis of Sailipu ultrapotassic rocks in southwestern Tibetan Plateau: constraints from zircon U-Pb geochronology and Hf isotopic compositions. *Acta Petrologica Sinica*, 24(02): 249~264 (in Chinese with English abstract).
- Tian Shihong, Hu Wenjie, Hou Zengqian, Mo Xuanxue, Yang Zhusen, Zhao Yue, Hou Kejun, Zhu Dichen, Su Aina, Zhang Zhaoqing. 2012. Enriched mantle source and petrogenesis of Miocene Sailipu ultrapotassic rocks in western Lhasa block, Tibetan Plateau: Lithium isotopic constraints. *Mineral Deposits*, 31(04): 791~812 (in Chinese with English abstract).

- Teng Fangzhen. 2017. Magnesium isotope geochemistry. *Reviews in Mineralogy and Geochemistry*, 82(1): 219~287.
- Teng Fangzhen, Li Wangye, Ke Shan, Marty B, Dauphas N, Huang Shichun, Wu Fuyuan, Pourmand A. 2010. Magnesium isotopic composition of the Earth and chondrites. *Geochimica et Cosmochimica Acta*, 74(14): 4150~4166.
- Teng Fangzhen, Li Wangye, Ke Shan, Yang Wei, Liu Shengao, Sedaghatpour F, Wang Shuijiong, Huang Kangjun, Hu Yan, Ling Mingxing, Xiao Yan, Liu Xiaoming, Li Xiaowei, Gu Haiou, Sio C K, Wallace D A, Su Benxun, Zhao Li, Chamberlin J, Harrington M, Brewer A. 2015. Magnesium isotopic compositions of international geological reference materials. *Geostandards and Geoanalytical Research*, 39(3): 329~339.
- Teng Fangzhen, Wadhwa M, Helz R T. 2007. Investigation of magnesium isotope fractionation during basalt differentiation: implications for a chondritic composition of the terrestrial mantle. *Earth and Planetary Science Letters*, 261(1): 84~92.
- Tommasini S, Avanzinelli R, Conticelli S. 2011. The Th/La and Sm/La conundrum of the Tethyan realm lamproites. *Earth and Planetary Science Letters*, 301(3): 469~478.
- Turner S, Arnaud N, Liu J, Rogers N, Hawkesworth C, Harris N, Kelley S, Calsteren P V, Deng W. 1996. Post-collisional shoshonitic volcanism on the Tibetan Plateau: Implications for convective thinning of the lithosphere and the source of ocean island basalts. *Journal of Petrology*, 37(1): 45~71.
- Valdes M C, Moreira M, Foriel J, Moynier F. 2014. The nature of Earth's building blocks as revealed by calcium isotopes. *Earth & Planetary Science Letters*, 394: 135~145.
- Wang Baodi, Chen Jianlin, Xu Jifeng, Wang Liquan. 2014. Geochemical and Sr-Nd-Pb-Os isotopic compositions of Miocene ultrapotassic rocks in southern Tibet: Petrogenesis and implications for the regional tectonic history. *Lithos*, 208: 237~250.
- Wang Shuijiong, Teng Fangzhen, Li Shuguang. 2014. Tracing carbonate-silicate interaction during subduction using magnesium and oxygen isotopes. *Nature Communications*, 5: 5328.
- Williams H M, Turner S P, Pearce J A, Kelley S P, Harris N B W. 2004. Nature of the source regions for post-collisional, potassic magmatism in southern and northern Tibet from geochemical variations and inverse trace element modelling. *Journal of Petrology*, 45(3): 555~607.
- Xiao Yan, Teng Fangzhen, Zhang Hongfu, Yang Wei. 2013. Large magnesium isotope fractionation in peridotite xenoliths from eastern North China craton: product of melt-rock interaction. *Geochimica et Cosmochimica Acta*, 115: 241~261.
- Xie Guogang, Zou Aijian, Yuan Jianya, Li Xiaoyong, Liao Siping, Tang Fenglin, Huang Chuanguan, Chen Zhenhua, Xu Zufeng. 2004. New results and major progress in regional geological survey of the Boindoi District and Comai sheets. *Geological Bulletin of China*, 23(5): 498~505 (in Chinese with English abstract).
- Xu Jifeng, Castillo P R. 2004. Geochemical and Nd-Pb isotopic characteristics of the Tethyan asthenosphere: implications for the origin of the Indian Ocean mantle domain. *Tectonophysics*, 393(1): 9~27.
- Xu Zhiqin, Wang Qin, Li Zhonghai, Li Huaqi, Cai Zihui, Liang Fenghua, Dong Hanwen, Cao Hui, Chen Xijie, Huang Xuemeng, Wu Chan, Xu Cuiping. 2016. Indo-Asian collision: Tectonic transition from compression to strike slip. *Acta Geologica Sinica*, 90(01): 1~23 (in Chinese with English abstract).
- Yang Wei, Teng Fangzhen, Zhang Hongfu. 2009. Chondritic magnesium isotopic composition of the terrestrial mantle: A case study of peridotite xenoliths from the North China craton. *Earth and Planetary Science Letters*, 288(3): 475~482.
- Yin An, Harrison T M. 2000. Geologic evolution of the Himalayan-Tibetan orogen. *Annual Review of Earth and Planetary Sciences*, 28(1): 211~280.
- Young E D, Galy A. 2004. The isotope geochemistry and cosmochemistry of magnesium. *Reviews in Mineralogy & Geochemistry*, 55: 197~230.
- Young E D, Tonui E, Manning C E, Schauble E, Macris C A. 2009. Spinel-olivine magnesium isotope thermometry in the mantle and implications for the Mg isotopic composition of Earth. *Earth and Planetary Science Letters*, 288(3): 524~533.
- Zhao Zhidan, Mo Xuanxue, Sebastien N, Paul R R, Zhou Su, Dong Guochen, Wang Liangliang, Zhu Dicheng, Liao Zhongli. 2006. Post-collisional ultrapotassic rocks in Lhasa Block, Tibetan Plateau: Spatial and temporal distribution and its implications. *Acta Petrologica Sinica*, 22(04): 787~794 (in Chinese with English abstract).
- Zhao Zhidan, Mo Xuanxue, Sun Chenguang, Zhu Dicheng, Niu Yaoling, Dong Guochen, Zhou Su, Dong Xin, Liu Yongsheng. 2008. Mantle xenoliths in southern Tibet: Geochemistry and constraints for nature of the mantle. *Acta Petrologica Sinica*, 24(2): 193~202 (in Chinese with English abstract).
- Zhao Zhidan, Mo Xuanxue, Dilek Yildirim, Niu Yaoling, Depaolo D J, Robinson P, Zhu Dicheng, Sun Chenguang, Dong Guochen, Zhou Su. 2009. Geochemical and Sr-Nd-Pb-O isotopic compositions of the post-collisional ultrapotassic magmatism in SW Tibet: Petrogenesis and implications for India intra-continental subduction beneath southern Tibet. *Lithos*, 113(1): 190~212.
- Zhu Dicheng, Zhao Zhidan, Niu Yaoling, Dilek Y, Hou Zengqian, Mo Xuanxue. 2013. The origin and pre-Cenozoic evolution of the Tibetan Plateau. *Gondwana Research*, 23(4): 1429~1454.
- Zhu Hongli, Zhang Zhao Feng, Wang Guiqin, Liu Yufei, Liu Fang, Li Xin, Sun Weidong. 2016. Calcium Isotopic Fractionation during Ion-Exchange Column Chemistry and Thermal Ionisation Mass Spectrometry (TIMS) Determination. *Geostandards and Geoanalytical Research*, 40(2): 185~194.

参 考 文 献

- 陈建林,许继峰,康志强,王保弟. 2007. 青藏高原西南部查孜地区中新世钾质火山岩地球化学及其成因. 地球化学, 36(05): 437~447.
- 陈建林,许继峰,康志强,王保弟. 2008. 青藏高原南部与北部新生代高镁钾质岩地球化学对比:南北地幔源区差异. 岩石学报, 24(02): 211~224.
- 丁林,岳雅慧,蔡福龙,徐晓霞,张清海,来庆洲. 2006. 西藏拉萨地块高镁超钾质火山岩及对南北向裂谷形成时间和切割深度的制约. 地质学报, 80(09): 1252~1261.
- 廖思平,陈振华,罗小川,邹爱建. 2002. 西藏当惹雍错地区白榴石响岩的发现及地质意义. 地质通报, 21(11): 735~738.
- 刘峪菲,祝红丽,刘芳,王桂琴,许继峰,张兆峰. 2015. 钙同位素化学分离方法研究. 地球化学, 44(05): 469~476.
- 孙晨光,赵志丹,莫宣学,朱弟成,董国臣,周肃,董昕,谢国刚. 2007. 青藏高原拉萨地块西部中新世赛利普超钾质岩石的地球化学与岩石成因. 岩石学报, 23(11): 2715~2726.
- 孙晨光,赵志丹,莫宣学,朱弟成,董国臣,周肃,陈海红,谢烈文,杨

- 岳衡,孙金凤,于枫. 2008. 青藏高原西南部赛利普超钾质火山岩富集地幔源区和岩石成因:锆石 U-Pb 年代学和 Hf 同位素制约. 岩石学报, 24(02): 249~264.
- 田世洪,胡文洁,侯增谦,莫宣学,杨竹森,赵悦,侯可军,朱弟成,苏媛娜,张兆卿. 2012. 拉萨地块西段中新世赛利普超钾质火山岩富集地幔源区和岩石成因:Li 同位素制约. 矿床地质, 31(04): 791~812.
- 谢国刚,邹爱建,袁建芽,李晓勇,廖思平,唐峰林,黄传冠,陈振华,徐祖丰. 2004. 邦多区幅、措麦区幅地质调查新成果及主要进展. 地质通报, 23(5): 498~505.
- 许志琴,王勤,李忠海,李化启,蔡志慧,梁凤华,董汉文,曹汇,陈希节,黄学猛,吴婵,许翠萍. 2016. 印度—亚洲碰撞:从挤压到走滑的构造转换. 地质学报, 90(01): 1~23.
- 赵志丹,莫宣学,Sebastien N,Paul R R,周肃,董国臣,王亮亮,朱弟成,廖忠礼. 2006. 青藏高原拉萨地块碰撞后超钾质岩石的时空分布及其意义. 岩石学报, 22(04): 787~794.
- 赵志丹,莫宣学,孙晨光,朱弟成,牛耀龄,董国臣,周肃,董昕,刘勇胜. 2008. 青藏高原南部地幔包体的发现及其意义. 岩石学报, 24(2): 193~202.

Ca-Mg Isotopic Compositions of Ultra-Potassic Volcanic Rocks in the Lhasa Terrane, Southern Tibet and Their Geological Implications

LIU Yafei^{1,2)}, XU Jifeng^{3,1)}, ZHANG Zhao Feng¹⁾, WANG Guiqin¹⁾, CHEN Jianlin¹⁾, HUANG Feng^{3,1)}, ZHU Hongli^{1, 2)}, LIU Fang^{1, 2)}

1) State Key Laboratory of Isotope Geochemistry, Guangzhou Institute of Geochemistry, Chinese Academy of Sciences, Guangzhou, 510640;

2) University of Chinese Academy of Sciences, Beijing, 100049;

3) School of Earth Sciences and Resources, China University of Geosciences, Beijing, 100083

Abstract

To better understand the compositions of enriched mantle source of ultra-potassic rocks in southern Tibet, here we report Ca and Mg isotopic compositions of eight ultra-potassic rock samples from the Mibale and Maiga areas in the Lhasa Terrane. Excluding the effect of weathering, crustal contamination, fractional crystallization and partial melting on ultra-potassic rocks' Ca and Mg isotopic compositions, it is determined that some carbonate sediments from subducted Neo-Thethyan oceanic crust may join into the mantle source of ultra-potassic rocks. The ultra-potassic rocks show significantly lower $\delta^{44}\text{Ca}$ values ranging from 0.59 to 0.75 (average = 0.68 ± 0.04), which are distinctly lower than the upper mantle (1.05 ± 0.04), bulk silicate earth (0.94 ± 0.05) and igneous rocks (0.80 ± 0.10). All these features indicate that the mantle source of ultra-potassic rocks might contain materials with low $\delta^{44}\text{Ca}$ value. The $\delta^{26}\text{Mg}$ values of ultra-potassic rocks display limited variation from -0.33 to -0.24 (mean = -0.29 ± 0.03), which are similar to the upper mantle ($\delta^{26}\text{Mg} = -0.25 \pm 0.07$) within the analytical uncertainty. The Ca-Mg isotopic compositions of ultra-potassic rocks are positively correlated, indicating their source might be metasomatized by the materials with low $\delta^{44}\text{Ca}$ and $\delta^{26}\text{Mg}$ value. Considering the tectonic evolution of Lhasa Terrane, we suggest that the low Ca-Mg isotopic materials are very likely marine carbonate sediments derived from subducted Neo-Tethyan oceanic crust.

Key words: Lhasa Terrane; ultra-potassic rocks; Ca-Mg isotopic composition; Mantle source; Tethyan subduction